HHS Public Access

Author manuscript

Annu Rev Biochem. Author manuscript; available in PMC 2022 June 20.

Published in final edited form as:

Annu Rev Biochem. 2021 June 20; 90: 559–579. doi:10.1146/annurev-biochem-071520-112507.

Membrane exporters of fluoride ion

Benjamin C. McIlwain[1], **Michal T. Ruprecht**[1], **Randy B. Stockbridge**[*,1,2]

[1]Department of Molecular, Cellular, and Developmental Biology, University of Michigan, Ann Arbor, MI 48109, USA

[2]Program in Biophysics, University of Michigan, Ann Arbor, MI 48109, USA

Abstract

Microorganisms contend with numerous and unusual chemical threats, and have evolved a catalogue of resistance mechanisms in response. One particularly ancient, pernicious threat is posed by fluoride ion (F^-), a common xenobiotic in natural environments that causes broad-spectrum harm to metabolic pathways. This review focuses on advances in the last ten years in understanding the microbial response to cytoplasmic accumulation of F^-, with a special emphasis on the structure and mechanisms of the proteins that microbes use to export fluoride, the CLC^F family of F^-/H^+ antiporters, and the Fluc/FEX family of F^- channels.

Keywords

fluoride; Fluc; FEX; CLC; ion channel; antiporter; membrane protein

INTRODUCTION

Nearly all microorganisms possess membrane proteins dedicated to the export of fluoride ion (F^-). These proteins belong to one of two families, each with a completely different fold, and that export F^- via fundamentally different mechanisms. The first group is a fluoride-specialized variant of the well-known CLC family (**Cl**$^-$ **c**hannel) of anion transporters and channels, called the CLC^Fs. These proteins are secondary active transporters that harness the proton motive force to export F^- in exchange for H^+ import(1). The second family, called Fluc (**Flu**oride **c**hannel) in bacteria and FEX (**F**luoride **ex**porter) in eukaryotes, are dedicated fluoride channels that permit electrodiffusive export of F^- (2, 3). In the extensive catalogue of ion channels and transporters, these are the first fluoride handling proteins to be identified. Moreover, they draw a stark contrast with most cases of fluoride complexation by biological macromolecules, in that they bind F^- without the aid of any metal ion.

Why are the CLC^Fs and Flucs so broadly distributed among microbes, and how do they work? This review will first address the biological rationale for fluoride export, including where microbes encounter fluoride, why intracellular fluoride accumulation is harmful, and

*To whom correspondence should be addressed. stockbr@umich.edu. Telephone: 734-764-3631.

Disclosure statement: The authors are not aware of any affiliations, memberships, funding, or financial holdings that might be perceived as affecting the objectivity of this review.

the mechanisms that microbes have evolved to mitigate this threat. We will then discuss the physicochemical features that distinguish fluoride from other common biological anions, and the molecular mechanisms by which the CLC^F and Fluc/FEX proteins exploit these differences to accomplish selective fluoride binding and export.

FLUORIDE IN THE BIOSPHERE

Environmental fluoride and weak acid accumulation

Fluoride ion has been abundant in the environment over evolutionary time (Figure 1a). Approximately 85 million tons of fluoride is concentrated in the earth's mantle, and volcanic eruptions disperse hydrofluoric acid (HF) and H_2SiF_4 volatiles that can settle in soil or water. This halide is commonly found in groundwater, where leaching of rocks containing fluoride-rich minerals, such as fluorite, apatite, and muscovite, deposits F^- to aquifers. Clay soils are also abundant in F^-, where the ion is often found in complex with cations like aluminum (Al^{3+})(4, 5). Natural environmental fluoride concentrations vary widely depending on the local geology, and range from 30–80 μM in oceans, and from 10 μM - 400 μM in ground and surface waters(4, 6). In some areas, human activity further increases ambient F^- concentrations over environmental levels. Fluoridation of municipal water supplies in the United States sets the F^- concentration of drinking water to ~40 μM in many locations (7), and F^- concentrations are higher still in areas affected by industrial pollution or by use of fluoride-contaminated fertilizers; and in niches such as the oral microbiome, where exposure to fluoride for dental hygiene – the concentration of fluoride ion is ~70 mM in toothpaste – is routine(4, 8).

Thus, broadly dispersed microbes frequently encounter fluoride in their environment. Exposure to this halide is further exacerbated in acidic niches (Figure 1b). The conjugate acid HF is a weak acid (pK_a = 3.4), and because HF is small and uncharged, it readily crosses the plasma membrane (9, 10). Since microbes maintain their cytoplasm at a constant pH between 7 and 7.5, even during mild acid stress(11, 12), HF that crosses the plasma membrane encounters a relatively higher cytoplasmic pH, which shifts the equilibrium towards dissociation to a proton and fluoride ion. These charged species cannot diffuse back across the membrane out of the cell, and thus accumulate, a process known as weak acid accumulation, or ion-trapping(13). In microbes that lack any F^- export pathway, intracellular F^- accumulates according to this simple scheme:

$$\frac{[F^-]_{in}}{[F^-]_{out}} = \frac{[H^+]_{out}}{[H^+]_{in}} \quad \text{(Eq. 1)}$$

so that for a microbe in a modestly acidic niche of pH 5.5 that maintains a cytoplasmic pH of 7.5, the intracellular fluoride will accumulate 100-fold in the cytoplasm compared to environmental levels, reaching millimolar concentrations (14).

F^- inhibition of biomolecules

Once it has breached the membrane and accumulated within the cell, fluoride is detrimental to biological systems because of its ability to act as substrate or transition state analogues for

a host of metalloenzymes involved in the most fundamental biological processes, ranging from glycolysis to nitrogen fixation to macromolecule synthesis(13, 15, 16). One common theme of enzyme inhibition by F^- is that the electronegative F^- effectively outcompetes electronegative substrate groups, such as OH^-, phosphate, or carboxylate, for coordination by an enzyme-bound metal ion. For example, in pyrophosphatase, F^- displaces the hydrolytic water in the coordination sphere of the enzyme-bound Mg^{2+}, acting as a transition state analogue of the activated water molecule(17, 18) (Figure 2a). In enolase, the enzyme that catalyzes the conversion of 2-phosphoglycerate to phosphoenolpyruvate during glycolysis, fluoride complexes an active site Mg^{2+}, displacing the substrate's carboxylate group(19–22) (Figure 2b). Enzymes that catalyze phosphoryl group transfer reactions, including kinases and other ATP-consuming enzymes, are also subject to inhibition by fluoride-metal ion complexes like the trigonal planar aluminium trifluoride (AlF_3) adduct, which behaves as a transition state analogue for phosphoryl group transfer reactions, or beryllium trifluoride (BeF_3^-), which mimics the geometry of a phosphate and forms a ground state analogue together with ADP(23, 24) (Figure 2c). Since aluminium is also found at physiologically relevant concentrations in soils, aluminium fluoride inhibition of phosphoryl group transfer enzymes is a germane biological phenomenon (4). In these various examples, the inhibitory constants by F^- are in the hundreds of micromolar range, well within the range of cytoplasmic F^- accumulation that occurs in modestly acidic environmental niches(14).

Biological response to F^- toxicity

Given the broad-spectrum sensitivity of metabolic processes to inhibition by fluoride, it is perhaps unsurprising that microbes possess mechanisms to mitigate the threat. However, the existence of the microbial fluoride response was unknown until 2012, when Ronald Breaker and colleagues showed that the conserved *crcB* riboswitch motif (Figure 2d), present in all domains of life, acts as a transcriptional "on-switch" upon fluoride ion binding(25). (See sidebar). Genes commonly associated with bacterial fluoride riboswitches (Figure 2e) include fluoride-sensitive metalloenzymes like enolase and the ATP-consuming DNA repair enzyme MutS shown in Figure 2. Na^+/H^+ antiporter genes also frequently co-occur with fluoride riboswitches. Because they help maintain pH homeostasis, the Na^+/H^+ antiporters may alleviate proton accumulation that occurs when HF enters the cell and dissociates. But the most frequently encountered genes, present in nearly half of all fluoride-riboswitch controlled operons, encode membrane proteins that have since been identified as fluoride ion exporters, the CLC^F (**CLC-F**luoride) and Fluc (**Flu**oride **c**hannel) proteins (Figure 2f).

By providing a route for accumulating F^- to exit the cell, expression of these F^- export proteins in the plasma membrane simply undermines weak acid accumulation of fluoride (1, 14, 25, 26). An extra thermodynamic push is provided by the proton motive force that metabolizing cells maintain. The CLC^Fs harness the proton gradient directly, by coupling fluoride export to proton import(1). For the Flucs, the positive-outside electrical potential thermodynamically favors anion expulsion (2). Although CLC^F and Fluc are unrelated by sequence, structure, and mechanism, their physiological roles overlap, and most bacteria have one or the other, but not both. Fluoride exporters from the CLC^F and Fluc families are

not necessarily associated with a riboswitch(1, 25); some, including the *E. coli* Fluc channel, are instead constitutively expressed (14).

CHALLENGES IN FLUORIDE RECOGNITION

The common challenge shared – and met – by the CLC^{F}s and the Flucs is to rapidly export F^-, but to do so with high specificity. Other anions like chloride (Cl^-) are more abundant in the cytoplasm (10–100 mM in *E. coli*(27)), and even low levels of uncontrolled leak would disrupt the membrane potential with catastrophic consequences for processes that rely on the electrical potential, including ATP synthesis, secondary active transport, and motility. However, specificity cannot be achieved by tight binding, since ionic throughput is a critical functional feature of transport proteins. And in contrast to the majority of F^- binding macromolecules, including those shown in Figure 2a–d, neither membrane exporter employs metal ions to bind or transport F^-, providing rare examples of biological F^- coordination without intervening metals.

Among the halides, F^- and Cl^- are the most similar, and, in synthetic applications, discriminating these anions has proved to be quite difficult, particularly in aqueous contexts(35, 36). F^- is the smallest of the halides, with a radius about half an Angstrom smaller than Cl^- (28). As such, F^- also has a higher charge density than Cl^-, and is therefore an especially strong hydrogen bond acceptor. This is reflected in the high energetic cost to dehydrate fluoride, 111 kcal/mol, approximately 30 kcal/mol more costly than dehydration of Cl^- (29). Because the F^- ions are dehydrated for transport, this energetic barrier must be surmounted. Theoretical treatments of halides show that inner sphere fluoride-water interactions are dominated by classical hydrogen bonds(37, 38), which are more tightly structured and closely held(33). In contrast, larger halides including Cl^- are more polarizable(30). Their coordination sphere is more flexible, and both hydrogen bond and dipole-dominated configurations occur(38). F^- prefers approximately one-two fewer ligands than Cl^- (31–34), and small molecule hosts designed for fluoride recognition commonly utilize between four and six hydrogen bond donors (32). Another unique aspect of fluoride is that it is a stronger base than the other halides and pseudohalides (and its conjugate acid, HF, a weaker acid). Whereas anions such as Cl^- and NO_3^- are exclusively ionized in aqueous media, the relatively high pK_a of HF means that this species may have relevance in biological systems, as it does in host-guest chemistry(10, 32). HF formation is particularly significant in low-dielectric environments such as the protein interior, where a fluoride ion might share a proton with pK_a-matched sidechains like aspartate or glutamate.

Thus, fluoride recognition by proteins is challenging due to the close size of prominent biological competitors and the especially high free energy of dehydration. But there are also a number of physicochemical properties that membrane transport proteins could exploit to differentiate F^- from Cl^-, including the preference of fluoride for fewer ligands and a tighter coordination shell, its greater strength as a hydrogen bond acceptor, and its unique ability to share protons with pK_a-matched protonatable sidechains.

CLC^F F^-/H^+ ANTIPORTERS

When the fluoride riboswitches and associated genes were discovered, the CLC (Cl^- channel) family of anion transport proteins was already well-known to biology. The CLC family comprises both anion channels and proton-coupled transporters, and are broadly distributed among nearly all organisms and cell types. CLCs play diverse physiological roles ranging from extreme acid resistance in bacteria, acidification of intracellular vesicles in eukaryotes, maintenance of the resting membrane potential of skeletal muscle and solute concentration in the kidney in animals, and generation of the voltage that electric rays use to electrocute their prey(39, 40). Although Cl^- is the namesake of the family, and in most cases the physiological ion, the canonical CLC proteins are not very selective among anions and also permeate other halides and pseudohalides like iodide, bromide, or nitrate(41). A number of Cl^- transporting CLCs have been structurally characterized, providing a deep mechanistic basis for understanding the fluoride riboswitch-associated CLCs (42–46).

The riboswitch-associated CLC proteins cluster together in a single bacterial clade of the CLC phylogeny(25). Not all proteins in this clade are associated with a riboswitch, but representatives with and without riboswitches share basic transport properties, and the proteins in this clade were thus renamed CLC^{F}s(1). When heterologously expressed, CLC^F representatives from both gram-negative and gram-positive bacteria protect *Escherichia coli* against fluoride toxicity (1). Genes encoding proteins in the CLC^F clade are overexpressed in fluoride-resistance *Streptococcus mutans* (47), upregulated in *Enterococcus faecalis* in response to fluoride stress(48) and deletion of the CLC^F genes severely impairs growth of the oral bacteria *S. mutans* and *Streptococcus anginosus* in fluoride-containing media(49). In addition, a number of homologues have been purified and characterized using *in vitro* transport and electrophysiological assays. The transporters harness the transmembrane proton gradient to export one F^- in exchange for one H^+, and the unitary transport rates of different characterized homologues ranges from ~400–1000 ions per second (1, 50). Sequence alignments show that proteins in the CLC^F clade lack many of the essential chloride-coordinating residues that are well-conserved in other chloride-transporting family members(1). In accord with this observation, the CLC^{F}s exhibit high selectivity for F^- relative to Cl^-, such that Cl^- permeation is not observed unless a high membrane potential is applied (1, 25, 50). Such selectivity is unique among CLCs, but makes good physiological sense: fluoride export is the only yet-described context in which a CLC must discriminate against molovalent anions that are more prevalent than the substrate in the biological milieu.

CLC^F structure and fluoride coordination

Like other CLC proteins, CLC^{F}s assemble as homodimers(51, 52). Each monomer contains the necessary machinery for ion permeation and proton-coupling, and if mutations are introduced that force the protein into a monomeric state, the lone subunits are capable of functioning independently(51). X-ray crystal structures of a CLC^F homologue from *Enterococcus casseliflavus*(52) show that each monomer possesses 14 transmembrane a-helices comprising two structurally homologous 7-helix domains that are related to one another by internal inverted symmetry (Figure 3a, 3b). In accordance with their role in anion transport, the a-helices are tilted with respect to the membrane, defining electropositive

internal and external aqueous vestibules that are 6–8 Å deep (Figure 3c). Breaks in these helices position the positive dipoles of the N-terminal ends of the helices near the central dehydrated anion-binding region of the protein, and also provide backbone amides to coordinate the transient anions (Figure 3d).

The crystal structures exhibit electron densities in two positions along the ion permeation pathway, termed the central (F_{cen}) and external (F_{ex}) anion binding sites (52) (Figure 3d). Although fluoride is isoelectronic with water, and thus indistinguishable by X-ray diffraction, these densities were assigned as fluoride ions by analogy to the well-characterized permeation pathway of other CLC proteins. The first of the fluoride binding sites, F_{cen}, sits at the apex of the cytoplasmic vestibule, where it is exposed to water and coordinated by protein sidechains in a manner reminiscent of other CLCs. In an interaction that has precedent in the Cl^- transporters (42), a sidechain hydroxyl from Y396 coordinates the fluoride. A methionine, M79, also contributes to F^- coordination via the terminal methyl group of the sidechain, which is polarized and rendered weakly electropositive by the adjacent electron-withdrawing sulfur. Mutagenesis experiments showed that this methionine contributes to F^-/Cl^- selectivity in the CLC^F proteins, and conversion to the straightforwardly polar asparagine reduces selectivity in a close homologue of the *E. casseliflavus* protein(50). The methionine is a somewhat surprising participant in fluoride coordination, since, in general, hard bases (like F^-) prefer coordination by hard acids, like conventional H-bond donors asparagine or serine(53). However, as will be described in the subsequent sections, F^- coordination by polarizeable amino acids, and methionine in particular, is reprised in the Fluc fluoride channels.

The second F^- binding site observed in the crystal structure, F_{ext}, is entirely dehydrated. This ion is coordinated by the sidechain of T320 along with backbone amides from consecutive residues, G116-G119, contributed by a helical break. In the structure of wildtype CLC^F, F^- ions occupy both the F_{cen} and the dehydrated F_{ext} site.

CLC^F fluoride transport mechanism and selectivity

In addition to the fluoride-coordinating residues, a final critical component of the transport machinery is the proton carrier, E118, which faces the external solution in the structure of the wildtype *E. casseliflavus* CLC^F. All members of the CLC family possess this so-called gating glutamate. In the CLC channels, the equivalent glutamate gates the conduction pathway depending on its protonation state(54), and in the CLC transporters, the glutamate participates in transport of the permeant H^+(55–57). The gating glutamate is likewise a key mechanistic player in the transport cycle of the CLC^F.

The CLC^F transport cycle proposed by Last, Miller, and colleagues(52), is based on competition between F^- and the negatively charged carboxylate of E118 for the binding sites F_{cen} and F_{ext} (Figure 4). In stage 1 of the transport cycle, the sidechain of the gating glutamate E118 is in the ‘up’ position, where it can obtain a proton from the extracellular milieu. Upon protonation, the now-neutral glutamate is proposed to swing down, following a hydrophobic pathway and bypassing the electropositive F^- binding sites (stage 2), so that it extends downward to access the *intracellular* vestibule, where it can release the bound proton

to the cytoplasm (stage 3). Such a conformationally swapped state, with E118 exposed to the internal solution, was captured in the crystal structure of a mutant transporter, V319G (52).

In the final phase of the transport cycle, having deposited its proton on the intracellular side, the now-negatively charged E118 outcompetes F^- for the F_{cen} site, chasing the bound F^- along the permeation pathway towards the extracellular solution. Deprotonated E118 is proposed to follow the F_{cen} ➔ F_{ext} ➔ external vestibule anion permeation route (stage 4), pushing a single F^- ahead of it, such that E118 transits back to the 'up' position in the extracellular vestibule. Thus, the excursions of this single sidechain carries a H^+ to the intracellular side, then electrostatically pushes a F^- to the extracellular side, providing a structural explanation for the 1-to-1 F^-/H^+ exchange stoichiometry. In accord with the proposal that electrostatic repulsion by the E118 carboxylate hastens F^- along the permeation pathway, F^- transport is abolished in neutral mutants E118Q and E118A – because the F^- binding affinity is over an order of magnitude *higher* in these mutants compared with wildtype(50, 52). In the absence of F^-, these mutants support Cl^- efflux, albeit uncoupled to H^+ exchange(52).

Compared with other CLC transporters, the aqueous vestibules of CLC^F are deeper and the anhydrous zone crossed by the permeant ions is shorter. This may be an adaptation to prevent unproductive interactions between the gating glutamate and the permeant F^-, which are close in pK_a and could conceivably capture a H^+ between them, especially when traversing a long, low-dielectric span. As a mechanistic counterpoint to the CLC^Fs, a bacterial Cl^-/H^+ CLC antiporter is potently inhibited when the protonated gating glutamate hydrogen bonds with a F^- in the anion binding site, "locking down" the glutamate and interrupting the transport cycle(58, 59). Thus, although the proteins CLC^Fs share many mechanistic features with the large CLC family of Cl^- transporters, both the anion binding sites and the interactions between the fluoride and the gating glutamate have been optimized for F^- transduction.

FLUC F^- CHANNELS

The second family of membrane proteins associated with the fluoride riboswitches is entirely dedicated to fluoride transport, and its members are unlike any previously characterized protein. Genes encoding these proteins, originally called *crcB*, are found not only in bacteria, but also in archaea, unicellular eukaryotes, fungi, plants, and filter feeding ocean animals like sponges and sea anemones. Electrophysiological characterization showed that the proteins encoded by the *crcB* genes are electrodiffusive F^- channels (2, 3, 60–63), and they were renamed Fluc (Fluoride channel) in bacteria and FEX (Fluoride exporter) in eukaryotes. Although it seems puzzling that a thermodynamically passive channel mechanism could protect organisms against external F^-, two factors favor fluoride export in the physiological context. First, the weak acid accumulation effect can lead to cytoplasmic fluoride levels that exceed external F^-, and a fluoride-selective efflux pathway simply undermines this process. Second, a metabolizing cell maintains a negative-inside membrane potential, so that the electrical potential favors anion expulsion(14).

In harmony with an electrodiffusive mechanism, single Fluc channels can be monitored in planar lipid bilayer electrophysiological recordings, where the fluoride conductances observed correspond to a throughput of ~$10^{5–6}$ ions/sec(2, 61). Unlike many gated channels, which open only in response to specific stimuli, the Fluc channels are constitutively open. The rapid fluoride conduction and lack of regulation poses a biophysical challenge, however: F^-/Cl^- selectivity of 100-fold, or even 1000-fold, would still permit an intolerable Cl^- leak. Accordingly, the Flucs are perhaps the most selective ion channels known; even low levels of Cl^- transport are not observed, placing the F^-/Cl^- selectivity at a minimum of 10,000-fold(2).

The protective role of the fluoride channels has been demonstrated in a broad array of organisms. Knockouts of genomic Fluc/FEX proteins increase fluoride sensitivity of bacteria including *Escherichia coli*(14, 25), *Bacillus subtilis*(25, 64), and oral bacterium *Streptococcus sanguinis*(49), and fungi including *Saccharomyces cerevisiae*(3, 26), *Candida albicans*(26), *Neurospora crassa*(26), and *Aspergillus fumigatus*(65). Moreover, proteins from plants and animals including *Arabidopsis thaliana*(66), the tea plant *Camellia sinensis*(67), and the sea sponge *Amphimedon queenslandica*(66) all complement strains of *S. cerevisiae* for which endogenous FEX channels have been knocked out.

Architecture of fluoride channels

The fluoride channel family encompasses a topologically diverse set of proteins that provide an unusual glimpse into evolutionary processes in membrane transport proteins(68) (Figure 5a). The eukaryotic FEX proteins, like the CLC^F proteins, have an inverted repeat architecture, in which two structurally homologous domains in a single polypeptide are arranged in opposite orientations(3, 26). Many other diverse membrane protein folds share this construction, which presumably arose from the duplication and fusion of a primal homodimer (69, 70). Remarkably, the bacterial Flucs embody this evolutionary antecedent, assembling as dual topology dimers, with one subunit inserted into the membrane with the termini facing out, and the other inserted into the membrane with the termini facing in (2, 60). Such an architecture is exceedingly rare among membrane proteins, and has only been structurally confirmed for two other transporter classes (71, 72). In addition to the dual topology homodimers, among bacterial Flucs, gene duplications have occurred on at least five occasions (68); the resultant protomers assemble as obligate antiparallel heterodimers where both subunits are required for channel assembly and function(2). The Flucs are the only functionally characterized family with modern-day representatives of all topological states along this evolutionary trajectory.

Of these various topologies, the dual topology homodimers, from *Bordetella pertussis* (Fluc-Bpe) and an *E. coli* virulence plasmid (Fluc-Ec2), are the only ones that have been structurally characterized(63, 73, 74). The Fluc fold is unique among known membrane proteins. The two 15-kDa subunits in the dimer, each composed of four transmembrane helices, adopt identical structures, such that the channels possess two-fold symmetry about an axis parallel to the plane of the membrane (Figure 5b). TM3 has a five-residue helical break that corresponds to one of the most highly conserved sequences in the protein. When the dimer is assembled, the TM3 breaks cross over each other at the heart of the protein,

where free backbone carbonyl oxygens coordinate a central sodium ion (Na^+) at the dimer interface (Figure 5c). This structural Na^+ ion is deeply buried, stably bound, and likely inserted upon dimer assembly(75). Although there is no known precedent among membrane proteins for such a non-transported structural Na^+, the binding site on the symmetry axis, coordinated by backbone carbonyl oxygens, resembles some Na^+ binding sites in Na^+-coupled transporters(75).

The channel adopts a symmetrical hourglass shape with wide aqueous vestibules on both sides of the membrane (Figure 5d). These vestibules are separated by a 10 Å thick protein plug that houses the structural Na^+. This Na^+, together with a universally conserved arginine residue, R22, render the vestibules electropositive, and both R22 and the Na^+ are essential for fluoride permeation(75). As a consequence of the dual topology architecture and two-fold symmetry, structural features that lie off the symmetry axis are found in duplicate. For example, the cytoplasmic and periplasmic faces of the channel are structurally identical. Functional experiments support this observation: an inhibitor applied in sequence to the *cis* and *trans* sides of a single Fluc channel in a planar lipid bilayer blocks both sides of the channel with identical kinetics (60–62). More strikingly, the channel also possesses a duplicate set of pores, each demarcated by a pair of fluoride ions arranged vertically, slightly off normal to the membrane plane (Figure 5c, 5e). Although the two-fold symmetry of the channels dictates that the two pores are antiparallel with respect to each other, electrophysiological experiments showed that fluoride uses both conduits to flow down its electrochemical gradient (76). However, inspection of the sequences of the heterodimeric and inverted-repeat fluoride channels suggests that both pores are not necessary. In the heterodimeric Fluc and FEX proteins, essential pore-lining residues are conserved in only one of the two domains(3, 66, 73), providing a case study in how redundant features degrade upon gene duplication, fusion, and genetic drift.

Fluc fluoride coordination and proposed permeation pathway

Using a combination of crystallographic and functional data from Fluc-Bpe and Fluc-Ec2, three different F^- binding sites have been proposed along the permeation pathway. Figures 6a and 6b illustrate the proposed pore, and are built from several different structures of the two homologues. Figure 6b posits a mechanism of alternating fluoride site occupancy, akin to that described for other multi-ion channels(77–81), where electrostatic repulsion between ions in adjacent sites contributes to rapid ion throughput. For simplicity, panels in Figure 6 show Fluc-Bpe unless otherwise indicated, residue numbering corresponds to Fluc-Bpe, and only one of the two structurally identical pores will be described.

Fluoride ions are proposed to accumulate in the electropositive vestibule, and in agreement with this, F^- currents are inhibited if the vestibule is occluded by the bulky, negatively charged thiol-reactive reagent MTSES (B.C. McIlwain, R. Gundepudi, B.B. Koff, and R.B. Stockbridge, manuscript in preparation). The first binding site along the permeation pathway, denoted F_0, is located at the bottom of the vestibule. This site is non-specific among anions, and was first identified by co-crystallization of Fluc-Ec2 with bromide (Br^-), a halide that anomalously scatters X-ray beams (B.C. McIlwain, R. Gundepudi, B.B. Koff, and R.B. Stockbridge, manuscript in preparation). An anion in the F_0 site is coordinated by

the sidechain hydroxyl groups of two highly conserved residues from the TM3 break, S83 and T84, along with bulk vestibule solvent. These positions are sensitive to mutagenesis: S83C and S83T are incompetent for F^- transport, and the double S83A/T84A mutant exhibits currents just 1% of wildtype (B.C. McIlwain, R. Gundepudi, B.B. Koff, and R.B. Stockbridge, manuscript in preparation). Such aqueous entryways are familiar features of ion channels more generally, and function to increase the rate of ion entry into the channel before the ions process to the constricted selectivity filter (82–84).

From F_0, the F^- ion is proposed to move laterally to access the fluoride-selective binding site F_1, which is located in an anhydrous crevice between TM2, TM3a, and TM4. F_1 and the next binding site in the series, F_2, delineate a pathway that runs perpendicular to the membrane along one face of TM4. Termed the polar track, this stretch of sequence is defined by a hydrogen bond donor at every fourth position, or one per helical turn (indicated with asterisks in Figure 6a). Sequences alignments show that although the identity of the polar track residues is not conserved among Fluc proteins, the polar, hydrogen-bond donating nature is (Figure 6c). In addition, TM2 contributes a completely conserved hydrogen bond donor, N43, to this polar, dehydrated stretch. N43 is situated between F_1 and F_2, with the sidechain amide coordinating F_2. A rotameric switch would bring this sidechain within coordination distance of F_1, and such an event was conjectured to be part of the transport mechanism(73). Alteration of N43 typically eliminates fluoride transport entirely (73, 85); the polar track residues, like the sidechains that coordinate F_0, are somewhat more tolerant of alanine substitution(85).

Along with this enrichment of hydrogen bond donors, the transient fluoride ions in the F_1 and F_2 positions are also coordinated by the electropositive edges of a pair of phenylalanines, F82 and F85 (Figure 6d). These highly conserved sidechains are arranged adjacent to the polar track in a symmetrical box configuration, with the electropositive edge of each Phe adjacent to the electronegative face of the next Phe. The polarizable aromatic rings are positioned to interact with the fluoride densities via side-on coordination by the electropositive quadrupoles of the ring edges. Such interactions, termed anion-quadrupole, have been observed in a variety of macromolecular contexts, and also occur between F^- and aromatic rings in small molecules (86–88). Mutation of either F82 or F85 to a non-polarizable hydrophobic residue like isoleucine greatly reduces or abolishes F^- transport, depending on the homologue(73, 76). Mutation to polar aromatic sidechains like tyrosine and tryptophan do not support transport either(85). However, mutation to methionine, which is, like phenylalanine, both hydrophobic and polarizable, supports fluoride conductance at wildtype levels (85). The structure of this mutant shows that the substituted methionine adopts a twisted conformation, filling approximately the same space as the Phe ring in the wildtype protein, with the electropositive g-methylene sitting in the same position as the Phe edge (Figure 6d). This interaction calls to mind the CLC^F's coordination of F_{cen} by a methionine, and in a handful of bacterial Fluc homologues, the phenylalanine box sequence motif includes a methionine instead(85).

After visiting sites F_0, F_1, and F_2, the permeant F^- is presumed to exit the pore on the other side of the membrane, near the mouth of the opposite vestibule. At this position resides a glutamate, E88. This glutamate is extremely well-conserved among fluoride channels and

follows the same pattern of conservation/degradation in the different domains of the eukaryotic channels as other pore-lining residues(73). In *S. cerevisiae* FEX channels, mutation of the corresponding glutamate renders the protein unprotective against F^-(66). Some evidence suggests that E88 contributes to anion selectivity, although its exact role is unclear. Analogy to the CLC^F proteins suggests the interesting hypothesis that E88 hastens F^- dissociation with an electrostatic push.

The unresolved question of fluoride selectivity by the Flucs

Although the permeation pathway has been determined, the features responsible for the striking 10,000-fold F^-/Cl^- selectivity have not yet been identified. Of dozens of mutations, none have allowed detectable throughput of any other anion, and increasing the bore of the channel by paring back sidechains has not yet been shown to decrease selectivity(73, 75, 76, 85). Because F^- requires the smallest number of coordinating ligands of any anion, it is plausible that only by *adding* ligands to the fluoride binding sites could the channel be engineered to bind other anions. Such a maneuver that would be difficult or impossible by site-directed mutagenesis alone. This type of selectivity mechanism, based on optimizing the number of protein ligands to coordinate the physiological ion and exclude competing ions, has been proposed for K^+ channels(89, 90) and as a general ion selectivity principle(33). The proposed fluoride binding sites in Fluc may be “under-coordinated,” with few protein ligands (three or four, assuming limited sidechain rearrangement) in order to exclude Cl^-. This sparsity of ligands in Fluc draws a contrast with the 5–6 ligands provided to each anion binding site by the less-selective CLC^Fs. It is also possible that rather than one selectivity filter, the Fluc channels have evolved multiple selectivity checkpoints, such that mutation to multiple regions of the protein would be required to permit chloride conduction. Or that some molecular feature – perhaps the hydrophobic polarizable sidechains – presents an insurmountable kinetic barrier to permeation by softer anions. Whatever the biophysical basis, the Flucs are impeccably optimized for fluoride selectivity and rapid conduction, all accomplished without any depletion of the microbe’s energy stores. It seems significant that the Fluc family has not evolved into a diversity of physiological roles like the CLCs: the Flucs are very specialized in what they do.

CONCLUSIONS

Nature has independently evolved two strikingly different fluoride export proteins to solve the problem of cytoplasmic fluoride accumulation. Not only do the proteins possess unrelated folds, it is highly unusual for the same biological problem to be solved by both passive and active transport mechanisms. Despite the very obvious differences in form and function, the CLC^F and Fluc proteins also share some common features. Some of these are expected, like the prevalence of hydroxyl sidechains as hydrogen bond donors for fluoride. Other common features are more surprising, like the involvement of hydrophobic polarizable sidechains methionine and phenylalanine in F^- coordination, and the occurrence of mechanistically important glutamate sidechains along the fluoride transport pathway. It remains to be determined whether the convergence of these features in the CLC^Fs and fluoride channels is evolutionary happenstance, or whether it reflects the unique suitability of these residues for fluoride conduction.

Sidebar: The fluoride riboswitch

The discovery of fluoride as the ligand for this riboswitch family by the Breaker lab was unexpected and serendipitous(25, 91). Searching for the natural ligand for this conserved RNA motif, riboswitch activation was observed upon the addition of various nucleotide substrates. But it wasn't nucleotide binding that threw the switch – the culprit turned out to be F^-, present at trace amounts from chemical synthesis(25). The apparent incongruence of a negative ion binding to a negatively charged RNA molecule has been resolved by structural studies(92, 93). Water molecules and five inwardly-pointing backbone phosphoryl groups coordinate three Mg^{2+} ions, which screen the negative charge. These Mg^{2+} ions, in turn, coordinate a single fluoride ion. The structure of the fluoride -Mg^{2+} nucleus is reminiscent of the fluoride-inhibited pyrophosphatase structure(17), with RNA phosphoryl groups in place of the substrate pyrophosphate.

Acknowledgements:

We thank members of the Stockbridge lab, especially Jason Devlin and Rachael Lucero, for comments on the manuscript. This work was supported by National Institutes of Health grant R35 GM128768 to RBS.

Terms and definitions:

Electrodiffusive
passive flow of an ion down its electrochemical gradient

Proton motive force (PMF)
the electrochemical proton gradient across the inner membrane; established by the electron transport chain

Dual topology
a membrane protein that is inserted into the membrane in both inward- and outward-facing orientations

Inverted repeat
two structurally homologous domains in a single polypeptide arranged with antiparallel topology

Riboswitch
a regulatory RNA element that alters gene transcription or translation in response to ligand binding

Anion-quadropole interaction
non-covalent interaction between an anion and the electron-deficient edge of an aromatic ring

Pseudohalide
a polyatomic anion that resembles the halides (fluoride, chloride, bromide, and iodide) in charge and chemical properties. Examples include nitrate, thiocyanate, cyanate, and azide.

Selectivity filter

the narrowest portion of an ion channel's conduction pathway that discriminates between ions.

Membrane potential
The difference in electrical potential across the membrane; a metabolizing bacterium typically has a negative-inside membrane potential of ~100 mV.

Helix dipole
the sum of amino acid dipoles renders the a-helix positive at the amino end and negative at the carboxy end.

Literature Cited:

1. Stockbridge RB, Lim HH, Otten R, Williams C, Shane T, et al. 2012. Fluoride resistance and transport by riboswitch-controlled CLC antiporters. Proc Natl Acad Sci U S A 109: 15289–94 [PubMed: 22949689]
2. Stockbridge RB, Robertson JL, Kolmakova-Partensky L, Miller C. 2013. A family of fluoride-specific ion channels with dual-topology architecture. Elife 2: e01084 [PubMed: 23991286]
3. Smith KD, Gordon PB, Rivetta A, Allen KE, Berbasova T, et al. 2015. Yeast Fex1p Is a Constitutively Expressed Fluoride Channel with Functional Asymmetry of Its Two Homologous Domains. Journal of Biological Chemistry 290: 19874–87
4. Weinstein LH, Davison A. 2004. Fluorides in the environment: effects on plants and animals. Cambridge, MA: CABI Publishing
5. Jagtap S, Yenkie MK, Labhsetwar N, Rayalu S. 2012. Fluoride in drinking water and defluoridation of water. Chem Rev 112: 2454–66 [PubMed: 22303811]
6. Windom HL. 1971. Fluoride Concentration in Coastal and Estuarine Waters of Georgia. Limnology and Oceanography 16: 806-&
7. Division of Oral Health: My Water's Fluoride web application. U.S. Department of Health and Human Services, Centers for Disease Control and Prevention (CDC), National Center for Chronic Disease Prevention and Health Promotion, Atlanta, GA, 2016. Available at http://www.cdc.gov/oralhealth/.
8. Johnston NR, Strobel SA. 2020. Principles of fluoride toxicity and the cellular response: a review. Archives of Toxicology 94: 1051–69 [PubMed: 32152649]
9. Barbier O, Arreola-Mendoza L, Del Razo LM. 2010. Molecular mechanisms of fluoride toxicity. Chem Biol Interact 188: 319–33 [PubMed: 20650267]
10. Orabi EA, Faraldo-Gomez JD. 2020. A New Molecular-Mechanics Model for Simulations of Hydrogen Fluoride in Chemistry and Biology. J Chem Theory Comput
11. Wilks JC, Slonczewski JL. 2007. pH of the cytoplasm and periplasm of Escherichia coli: rapid measurement by green fluorescent protein fluorimetry. J Bacteriol 189: 5601–7 [PubMed: 17545292]
12. Krulwich TA, Sachs G, Padan E. 2011. Molecular aspects of bacterial pH sensing and homeostasis. Nat Rev Microbiol 9: 330–43 [PubMed: 21464825]
13. Marquis RE, Clock SA, Mota-Meira M. 2003. Fluoride and organic weak acids as modulators of microbial physiology. FEMS Microbiol Rev 26: 493–510 [PubMed: 12586392]
14. Ji C, Stockbridge RB, Miller C. 2014. Bacterial fluoride resistance, Fluc channels, and the weak acid accumulation effect. The Journal of General Physiology 144: 257–61 [PubMed: 25156118]
15. Adamek E, Pawlowska-Goral K, Bober K. 2005. In vitro and in vivo effects of fluoride ions on enzyme activity. Ann Acad Med Stetin 51: 69–85 [PubMed: 16519100]
16. Johnston NR, Strobel SA. 2019. Nitrate and Phosphate Transporters Rescue Fluoride Toxicity in Yeast. Chemical Research in Toxicology 32: 2305–19 [PubMed: 31576749]

17. Samygina VR, Moiseev VM, Rodina EV, Vorobyeva NN, Popov AN, et al. 2007. Reversible inhibition of Escherichia coli inorganic pyrophosphatase by fluoride: trapped catalytic intermediates in cryo-crystallographic studies. J Mol Biol 366: 1305–17 [PubMed: 17196979]
18. Heikinheimo P, Tuominen V, Ahonen AK, Teplyakov A, Cooperman BS, et al. 2001. Toward a quantum-mechanical description of metal-assisted phosphoryl transfer in pyrophosphatase. Proceedings of the National Academy of Sciences of the United States of America 98: 3121–26 [PubMed: 11248042]
19. Qin J, Chai G, Brewer JM, Lovelace LL, Lebioda L. 2006. Fluoride inhibition of enolase: crystal structure and thermodynamics. Biochemistry 45: 793–800 [PubMed: 16411755]
20. Lebioda L, Zhang E, Lewinski K, Brewer JM. 1993. Fluoride inhibition of yeast enolase: crystal structure of the enolase-Mg(2+)-F(−)-Pi complex at 2.6 A resolution. Proteins 16: 219–25 [PubMed: 8346189]
21. Nowak T, Maurer PJ. 1981. Fluoride inhibition of yeast enolase. 2. Structural and kinetic properties of the ligand complexes determined by nuclear relaxation rate studies. Biochemistry 20: 6901–11 [PubMed: 7032583]
22. Maurer PJ, Nowak T. 1981. Fluoride inhibition of yeast enolase. 1. Formation of the ligand complexes. Biochemistry 20: 6894–900 [PubMed: 7032582]
23. Matte A, Tari LW, Delbaere LT. 1998. How do kinases transfer phosphoryl groups? Structure 6: 413–9 [PubMed: 9562560]
24. Alani E, Lee JY, Schofield MJ, Kijas AW, Hsieh P, Yang W. 2003. Crystal structure and biochemical analysis of the MutS.ADP.beryllium fluoride complex suggests a conserved mechanism for ATP interactions in mismatch repair. J Biol Chem 278: 16088–94 [PubMed: 12582174]
25. Baker JL, Sudarsan N, Weinberg Z, Roth A, Stockbridge RB, Breaker RR. 2012. Widespread genetic switches and toxicity resistance proteins for fluoride. Science 335: 233–5 [PubMed: 22194412]
26. Li S, Smith KD, Davis JH, Gordon PB, Breaker RR, Strobel SA. 2013. Eukaryotic resistance to fluoride toxicity mediated by a widespread family of fluoride export proteins. Proceedings of the National Academy of Sciences 110: 19018–23
27. Schultz SG, Wilson NL, Epstein W. 1962. Cation transport in Escherichia coli. II. Intracellular chloride concentration. J Gen Physiol 46: 159–66 [PubMed: 13909522]
28. Shannon RD. 1976. Revised effective ionic radii and systematic studies of interatomic distances in halides and chalcogenides. Acta Crystallogr A 32: 751–67
29. Marcus Y 1994. A Simple Empirical-Model Describing the Thermodynamics of Hydration of Ions of Widely Varying Charges, Sizes, and Shapes. Biophysical Chemistry 51: 111–27
30. Li M, Zhuang B, Lu Y, Wang ZG, An L. 2017. Accurate Determination of Ion Polarizabilities in Aqueous Solutions. J Phys Chem B 121: 6416–24 [PubMed: 28594180]
31. Ohtaki H, Radnai T. 1993. Structure and Dynamics of Hydrated Ions. Chemical Reviews 93: 1157–204
32. Cametti M, Rissanen K. 2013. Highlights on contemporary recognition and sensing of fluoride anion in solution and in the solid state. Chem Soc Rev 42: 2016–38 [PubMed: 23188119]
33. Bostick DL, Brooks CL. 2009. Statistical Determinants of Selective Ionic Complexation: Ions in Solvent, Transport Proteins, and Other “Hosts”. Biophysical Journal 96: 4470–92 [PubMed: 19486671]
34. Merchant S, Asthagiri D. 2009. Thermodynamically dominant hydration structures of aqueous ions. Journal of Chemical Physics 130
35. Cametti M, Rissanen K. 2009. Recognition and sensing of fluoride anion. Chem Commun (Camb): 2809–29 [PubMed: 19436879]
36. Clarke HJ, Howe EN, Wu X, Sommer F, Yano M, et al. 2016. Transmembrane Fluoride Transport: Direct Measurement and Selectivity Studies. J Am Chem Soc 138: 16515–22 [PubMed: 27998094]
37. Muralidharan A, Pratt LR, Chaudhari MI, Rempe SB. 2018. Quasi-Chemical Theory with Cluster Sampling from Ab Initio Molecular Dynamics: Fluoride (F(−)) Anion Hydration. J Phys Chem A 122: 9806–12 [PubMed: 30475612]

38. Muralidharan A, Pratt LR, Chaudhari MI, Rempe SB. 2019. Quasi-chemical theory for anion hydration and specific ion effects: Cl-(aq) vs. F-(aq). Chemical Physics Letters: X 4: 100037
39. Jentsch TJ, Pusch M. 2018. CLC Chloride Channels and Transporters: Structure, Function, Physiology, and Disease. Physiol Rev 98: 1493–590 [PubMed: 29845874]
40. Miller C 2015. In the beginning: a personal reminiscence on the origin and legacy of ClC-0, the 'Torpedo Cl(−) channel'. J Physiol 593: 4085–90 [PubMed: 25433078]
41. Accardi A, Lobet S, Williams C, Miller C, Dutzler R. 2006. Synergism between halide binding and proton transport in a CLC-type exchanger. J Mol Biol 362: 691–9 [PubMed: 16949616]
42. Dutzler R, Campbell EB, Cadene M, Chait BT, MacKinnon R. 2002. X-ray structure of a ClC chloride channel at 3.0 A reveals the molecular basis of anion selectivity. Nature 415: 287–94 [PubMed: 11796999]
43. Jayaram H, Accardi A, Wu F, Williams C, Miller C. 2008. Ion permeation through a Cl--selective channel designed from a CLC Cl−/H+ exchanger. Proc Natl Acad Sci U S A 105: 11194–9 [PubMed: 18678918]
44. Feng L, Campbell EB, Hsiung Y, MacKinnon R. 2010. Structure of a eukaryotic CLC transporter defines an intermediate state in the transport cycle. Science 330: 635–41 [PubMed: 20929736]
45. Park E, Campbell EB, MacKinnon R. 2017. Structure of a CLC chloride ion channel by cryo-electron microscopy. Nature 541: 500–05 [PubMed: 28002411]
46. Park E, MacKinnon R. 2018. Structure of the CLC-1 chloride channel from Homo sapiens. Elife 7
47. Liao Y, Chen J, Brandt BW, Zhu Y, Li J, et al. 2015. Identification and functional analysis of genome mutations in a fluoride-resistant Streptococcus mutans strain. PLoS One 10: e0122630 [PubMed: 25856576]
48. Li G, Shi M, Zhao S, Li D, Long Y, et al. 2020. RNA-Seq comparative analysis reveals the response of Enterococcus faecalis TV4 under fluoride exposure. Gene 726: 144197 [PubMed: 31669636]
49. Men X, Shibata Y, Takeshita T, Yamashita Y. 2016. Identification of Anion Channels Responsible for Fluoride Resistance in Oral Streptococci. PLoS One 11: e0165900 [PubMed: 27824896]
50. Brammer AE, Stockbridge RB, Miller C. 2014. F−/Cl− selectivity in CLCF-type F−/H+ antiporters. J Gen Physiol 144: 129–36 [PubMed: 25070431]
51. Last NB, Miller C. 2015. Functional Monomerization of a ClC-Type Fluoride Transporter. J Mol Biol 427: 3607–12 [PubMed: 26449639]
52. Last NB, Stockbridge RB, Wilson AE, Shane T, Kolmakova-Partensky L, et al. 2018. A CLC-type F(−)/H(+) antiporter in ion-swapped conformations. Nat Struct Mol Biol
53. Pearson RG. 1966. Acids and bases. Science 151: 172–7 [PubMed: 17746330]
54. Lisal J, Maduke M. 2008. The ClC-0 chloride channel is a 'broken' Cl−/H+ antiporter. Nat Struct Mol Biol 15: 805–10 [PubMed: 18641661]
55. Feng L, Campbell EB, MacKinnon R. 2012. Molecular mechanism of proton transport in CLC Cl −/H+ exchange transporters. Proc Natl Acad Sci U S A 109: 11699–704 [PubMed: 22753511]
56. Dutzler R, Campbell EB, MacKinnon R. 2003. Gating the selectivity filter in ClC chloride channels. Science 300: 108–12 [PubMed: 12649487]
57. Chavan TS, Cheng RC, Jiang T, Mathews II, Stein RA, et al. 2020. A CLC-ec1 mutant reveals global conformational change and suggests a unifying mechanism for the CLC Cl(−)/H(+) transport cycle. Elife 9
58. Lim HH, Stockbridge RB, Miller C. 2013. Fluoride-dependent interruption of the transport cycle of a CLC Cl−/H+ antiporter. Nat Chem Biol 9: 721–5 [PubMed: 24036509]
59. Chiariello MG, Bolnykh V, Ippoliti E, Meloni S, Olsen JMH, et al. 2020. Molecular Basis of CLC Antiporter Inhibition by Fluoride. Journal of the American Chemical Society 142: 7254–58 [PubMed: 32233472]
60. Stockbridge RB, Koide A, Miller C, Koide S. 2014. Proof of dual-topology architecture of Fluc F-channels with monobody blockers. Nat Commun 5: 5120 [PubMed: 25290819]
61. Turman DL, Nathanson JT, Stockbridge RB, Street TO, Miller C. 2015. Two-sided block of a dual-topology F- channel. Proc Natl Acad Sci U S A 112: 5697–701 [PubMed: 25902543]

62. Turman DL, Stockbridge RB. 2017. Mechanism of single- and double-sided inhibition of dual topology fluoride channels by synthetic monobodies. J Gen Physiol
63. McIlwain BC, Newstead S, Stockbridge RB. 2018. Cork-in-Bottle Occlusion of Fluoride Ion Channels by Crystallization Chaperones. Structure 26: 635–39 e1 [PubMed: 29526432]
64. Dong W, Setlow P. 2019. Fluoride movement into and out of Bacillus spores and growing cells and effects of fluoride accumulation on spore properties. J Appl Microbiol 126: 503–15 [PubMed: 30430725]
65. Binder J, Held J, Krappmann S. 2019. Impairing fluoride export of Aspergillus fumigatus mitigates its voriconazole resistance. Int J Antimicrob Agents 53: 689–93 [PubMed: 30763611]
66. Berbasova T, Nallur S, Sells T, Smith KD, Gordon PB, et al. 2017. Fluoride export (FEX) proteins from fungi, plants and animals are 'single barreled' channels containing one functional and one vestigial ion pore. PLoS One 12: e0177096 [PubMed: 28472134]
67. Zhu J, Xing A, Wu Z, Tao J, Ma Y, et al. 2019. CsFEX, a Fluoride Export Protein Gene from Camellia sinensis, Alleviates Fluoride Toxicity in Transgenic Escherichia coli and Arabidopsis thaliana. J Agric Food Chem 67: 5997–6006 [PubMed: 31056906]
68. Macdonald CB, Stockbridge RB. 2017. A topologically diverse family of fluoride channels. Curr Opin Struct Biol 45: 142–49 [PubMed: 28514705]
69. Forrest LR. 2015. Structural Symmetry in Membrane Proteins. Annu Rev Biophys 44: 311–37 [PubMed: 26098517]
70. Keller R, Ziegler C, Schneider D. 2014. When two turn into one: evolution of membrane transporters from half modules. Biol Chem 395: 1379–88 [PubMed: 25296672]
71. Ubarretxena-Belandia I, Baldwin JM, Schuldiner S, Tate CG. 2003. Three-dimensional structure of the bacterial multidrug transporter EmrE shows it is an asymmetric homodimer. EMBO J 22: 6175–81 [PubMed: 14633977]
72. Assur Sanghai Z, Liu Q, Clarke OB, Belcher-Dufrisne M, Wiriyasermkul P, et al. 2018. Structure-based analysis of CysZ-mediated cellular uptake of sulfate. Elife 7
73. Stockbridge RB, Kolmakova-Partensky L, Shane T, Koide A, Koide S, et al. 2015. Crystal structures of a double-barrelled fluoride ion channel. Nature 525: 548–51 [PubMed: 26344196]
74. Turman DL, Cheloff AZ, Corrado AD, Nathanson JT, Miller C. 2018. Molecular Interactions between a Fluoride Ion Channel and Synthetic Protein Blockers. Biochemistry
75. McIlwain BC, Martin K, Hayter EA, Stockbridge RB. 2020. An Interfacial Sodium Ion is an Essential Structural Feature of Fluc Family Fluoride Channels. J Mol Biol
76. Last NB, Kolmakova-Partensky L, Shane T, Miller C. 2016. Mechanistic signs of double-barreled structure in a fluoride ion channel. Elife 5
77. Morais-Cabral JH, Zhou Y, MacKinnon R. 2001. Energetic optimization of ion conduction rate by the K+ selectivity filter. Nature 414: 37–42 [PubMed: 11689935]
78. Hodgkin AL, Keynes RD. 1955. The Potassium Permeability of a Giant Nerve Fibre. Journal of Physiology-London 128: 61–88
79. Eisenman W 1962. A 2-Way Affair. Science 136: 182-&
80. Hille B, Schwarz W. 1978. Potassium Channels as Multi-Ion Single-File Pores. Journal of General Physiology 72: 409–42
81. Zhou YF, MacKinnon R. 2003. The occupancy of ions in the K+ selectivity filter: Charge balance and coupling of ion binding to a protein conformational change underlie high conduction rates. Journal of Molecular Biology 333: 965–75 [PubMed: 14583193]
82. Doyle DA, Morais Cabral J, Pfuetzner RA, Kuo A, Gulbis JM, et al. 1998. The structure of the potassium channel: molecular basis of K+ conduction and selectivity. Science 280: 69–77 [PubMed: 9525859]
83. Latorre R, Miller C. 1983. Conduction and Selectivity in Potassium Channels. Journal of Membrane Biology 71: 11–30 [PubMed: 6300405]
84. Payandeh J, Scheuer T, Zheng N, Catterall WA. 2011. The crystal structure of a voltage-gated sodium channel. Nature 475: 353–8 [PubMed: 21743477]
85. Last NB, Sun S, Pham MC, Miller C. 2017. Molecular determinants of permeation in a fluoride-specific ion channel. Elife 6

86. Philip V, Harris J, Adams R, Nguyen D, Spiers J, et al. 2011. A survey of aspartate-phenylalanine and glutamate-phenylalanine interactions in the protein data bank: searching for anion-pi pairs. Biochemistry 50: 2939–50 [PubMed: 21366334]

87. Allen FH. 2002. The Cambridge Structural Database: a quarter of a million crystal structures and rising. Acta Crystallographica Section B-Structural Science 58: 380–88

88. Chakravarty S, Ung AR, Moore B, Shore J, Alshamrani M. 2018. A Comprehensive Analysis of Anion-Quadrupole Interactions in Protein Structures. Biochemistry 57: 1852–67 [PubMed: 29482321]

89. Bostick DL, Brooks CL 3rd. 2007. Selectivity in K+ channels is due to topological control of the permeant ion's coordinated state. Proc Natl Acad Sci U S A 104: 9260–5 [PubMed: 17519335]

90. Varma S, Sabo D, Rempe SB. 2008. K+/Na+ selectivity in K channels and valinomycin: Over-coordination versus cavity-size constraints. Journal of Molecular Biology 376: 13–22 [PubMed: 18155244]

91. Sherlock ME, Breaker RR. 2020. Former orphan riboswitches reveal unexplored areas of bacterial metabolism, signaling, and gene control processes. RNA 26: 675–93 [PubMed: 32165489]

92. Zhao B, Guffy SL, Williams B, Zhang Q. 2017. An excited state underlies gene regulation of a transcriptional riboswitch. Nat Chem Biol 13: 968–74 [PubMed: 28719589]

93. Ren A, Rajashankar KR, Patel DJ. 2012. Fluoride ion encapsulation by Mg2+ ions and phosphates in a fluoride riboswitch. Nature 486: 85–9 [PubMed: 22678284]

94. Fernandez R, Berro J. 2016. Use of a fluoride channel as a new selection marker for fission yeast plasmids and application to fast genome editing with CRISPR/Cas9. Yeast 33: 549–57 [PubMed: 27327046]

95. Lellouche J, Friedman A, Gedanken A, Banin E. 2012. Antibacterial and antibiofilm properties of yttrium fluoride nanoparticles. Int J Nanomedicine 7: 5611–24 [PubMed: 23152681]

96. Li S, Breaker RR. 2012. Fluoride enhances the activity of fungicides that destabilize cell membranes. Bioorg Med Chem Lett 22: 3317–22 [PubMed: 22460034]

97. Nelson JW, Zhou Z, Breaker RR. 2014. Gramicidin D enhances the antibacterial activity of fluoride. Bioorg Med Chem Lett 24: 2969–71 [PubMed: 24857543]

98. Jurcik A, Bednar D, Byska J, Marques SM, Furmanova K, et al. 2018. CAVER Analyst 2.0: analysis and visualization of channels and tunnels in protein structures and molecular dynamics trajectories. Bioinformatics 34: 3586–88 [PubMed: 29741570]

Summary Points:

- Fluoride ion is ubiquitous in terrestrial and aquatic environment, and poses a threat to microbes because it can accumulate in the cytoplasm via a weak acid ion trapping mechanism, where it inhibits diverse metalloenzymes.
- Two strikingly different families of membrane protein export cytoplasmic fluoride: the CLC^F F^-/H^+ antiporters and the Fluc fluoride channels.
- CLC^F transporters are a fluoride-specialized variant of the ubiquitous CLC family of anion channels and transporters.
- The Fluc family is dedicated to F^- export, and have a unique structure among membrane proteins. However, fundamental aspects of its construction calls to mind features of long-studied ion channels, including the wide aqueous entryway (82–84), and multi-ion conduction (77–81).
- Although they are structurally unrelated, the CLC^Fs and Flucs share common features in their F^- permeation pathways, including coordination by hydrophobic polarizable amino acids such as methionine and phenylalanine, hydrogen bond donation by hydroxyl sidechains, and participation of conserved glutamate residues.

Future Issues:

- Additional mechanistic work, including both experimental and computational investigations, will be important to understand the contributions of polarizable amino acids to F^- binding, and the physicochemical basis of F^- selectivity, especially in the Flucs, for which no modification has yet been discovered that permits the permeation of any other anion.
- Eukaryotic FEX proteins have a fundamental architectural difference with the homodimeric Flucs. Structural characterization of eukaryotic FEX proteins will be important both to understand how eukaryotic pathogens resist environmental fluoride, as well as to answer more basic questions about how membrane proteins evolve in complexity upon duplication and fusion of the individual subunits.
- Identification of the microbial molecular response to fluoride has launched a new era in applied fluoride physiology, including use of fluoride channels as selectable markers in transgenic yeast (94), and the design of fluoride-centric antimicrobial approaches(95). Research is ongoing in a variety of organisms relevant to human disease in order to understand whether fluoride sensing and export systems are suitable drug targets, particularly in dental applications(65, 96, 97).
- It remains unknown whether higher animals possess fluoride export proteins. Although fluoride is not transported to the bloodstream by the excretory epithelia, epithelial cells in the gut are exposed to this halide, and the molecular physiology of these encounters, including any possible export systems, is yet unknown.

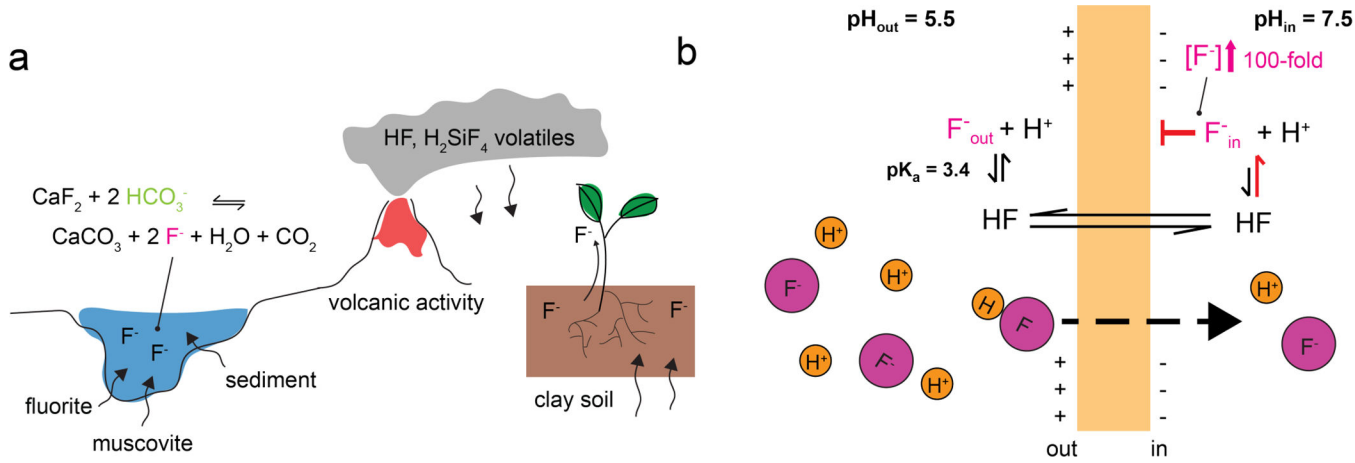

Figure 1. Environmental sources of aqueous and terrestrial fluoride and weak acid accumulation.

a. Alkaline environments rich in bicarbonate ion (HCO_3^-) promote exchange of F^- trapped in aquifer rocks. Volatile fluoride complexes are dispersed from deep within the earth's crust via volcanic activity, to the terrestrial surface where it is encountered by plants and microbes. b. Weak acid accumulation (ion-trapping) pathway for the intracellular accumulation of F^- in modestly acidic environmental niches. A 2-unit pH differential across the membrane leads to 100-fold elevation in intracellular fluoride over environmental levels according to Eq. 1.

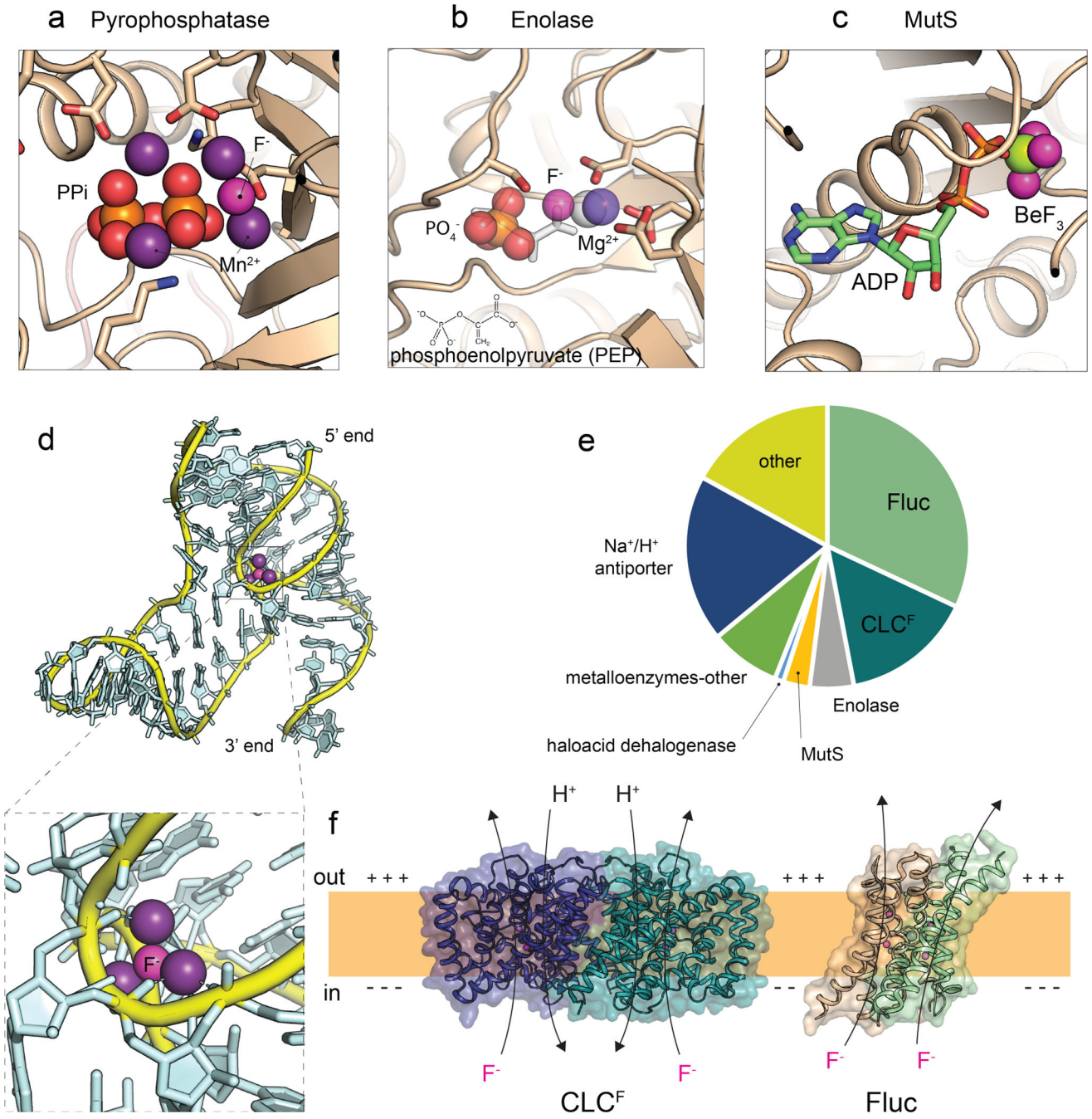

Figure 2. Biological response to cytoplasmic fluoride accumulation.

a.-c. Inhibition of enzymes by fluoride. F^- is shown as a pink sphere in each view. a. Pyrophosphatase (PDB: 1E6A). Pyrophosphate (PP_i) shown as orange/red spheres, and Mn^{2+} in violet. b. Enolase (PDB: 1NEL). The position of the natural product, phosphoenolpyruvate (transparent white sticks) complexed with Mg^{2+} (white sphere), is overlaid with the structure of the inhibitory $F^-/PO_4^-/Mn^{2+}$ complex (colored spheres: PO_4^- in red/orange and Mn^{2+} in violet). F^- binds in the same position as the carboxylate group of the substrate or product. c. The ATP-dependent DNA repair enzyme MutS (PDB: 1NNE)

with bound ADP (sticks) and BeF_3^- adduct (beryllium in light green and fluoride ion pink). Here, the BeF_3^- adduct mimics the terminal phosphoryl group of ATP. d. Structure of the fluoride-sensing riboswitch of *Thermotoga petrophila* (PDB: 4ENB). The fluoride ion is shown as a pink sphere, and magnesium ions are shown in violet. Lower panel: zoomed-in view of fluoride binding site. e. Genetic association of fluoride-sensitive enzymes and fluoride exporters with fluoride riboswitches. Pie graph adapted from ref. (25). Sections are proportional to the number of bacterial operons that encode each protein. f. Riboswitch-associated fluoride exporters CLC^F and Fluc (PDB: 6D0J, 5NKQ). The membrane is indicated by the orange slab, with typical membrane polarization shown with (+) and (−) symbols. The direction of ion movement is shown for each protein.

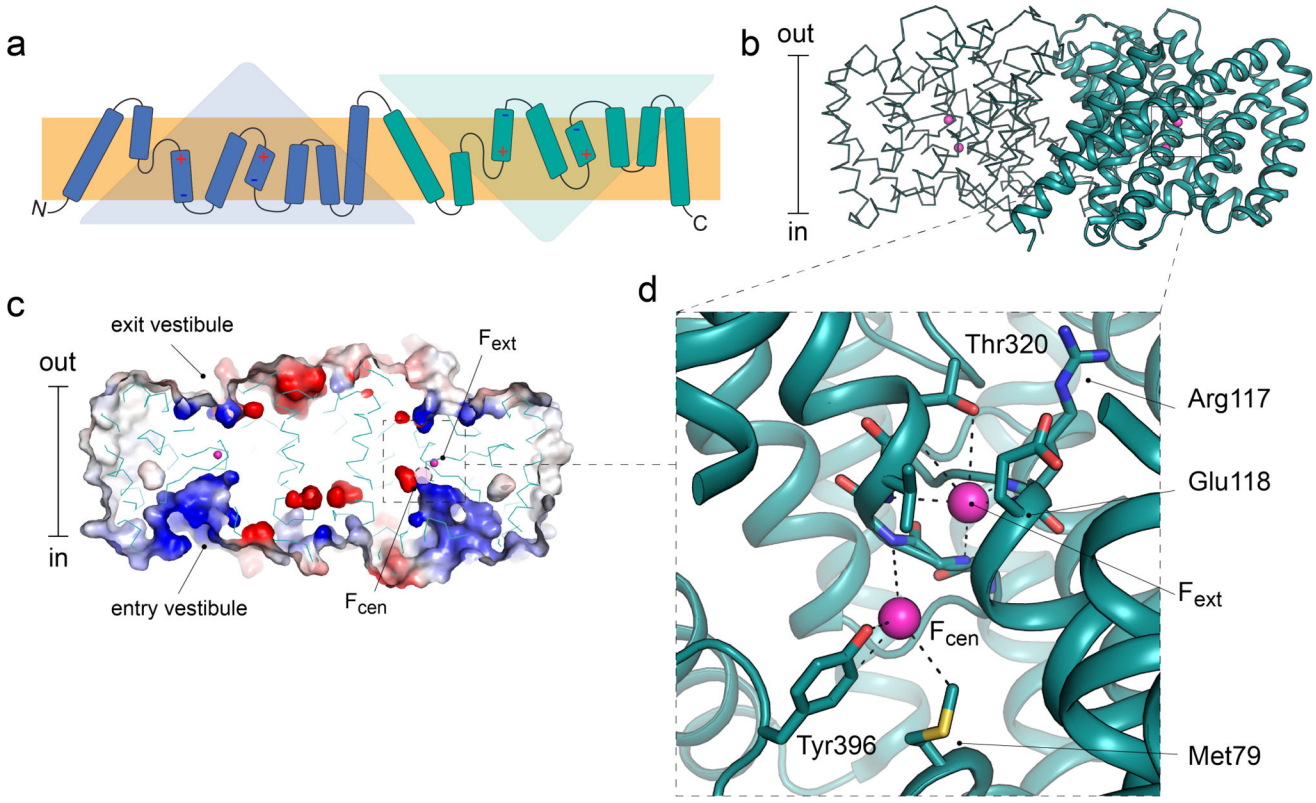

Figure 3. CLC^F architecture and F$^-$ binding.

a. Transmembrane topology of a single subunit of the CLC^F dimer. The two domains of the inverted repeat are colored blue and teal. b. Three-dimensional structure of the CLC^F dimer from *Enterococcus casseliflavus* (PDB: 6D0J) with bound fluoride ions and approximate membrane boundaries shown. c. Sideview of CLC^F dimer, sliced along a plane perpendicular to the membrane at the protein center, with electrostatic surface shown. Blue regions are electropositive, and red regions are electronegative. Fluoride ions at the F_{ext} position are shown as pink spheres. Fluoride ions at the F_{cen} position are not visible in this slice; their approximate location at the top of the intracellular vestibule is indicated by the dashed circle. d. Detailed view of fluoride binding at F_{cen} and F_{ext}. Amino acids within hydrogen bond distance are shown as sticks, with potential hydrogen bonds shown as dashed lines.

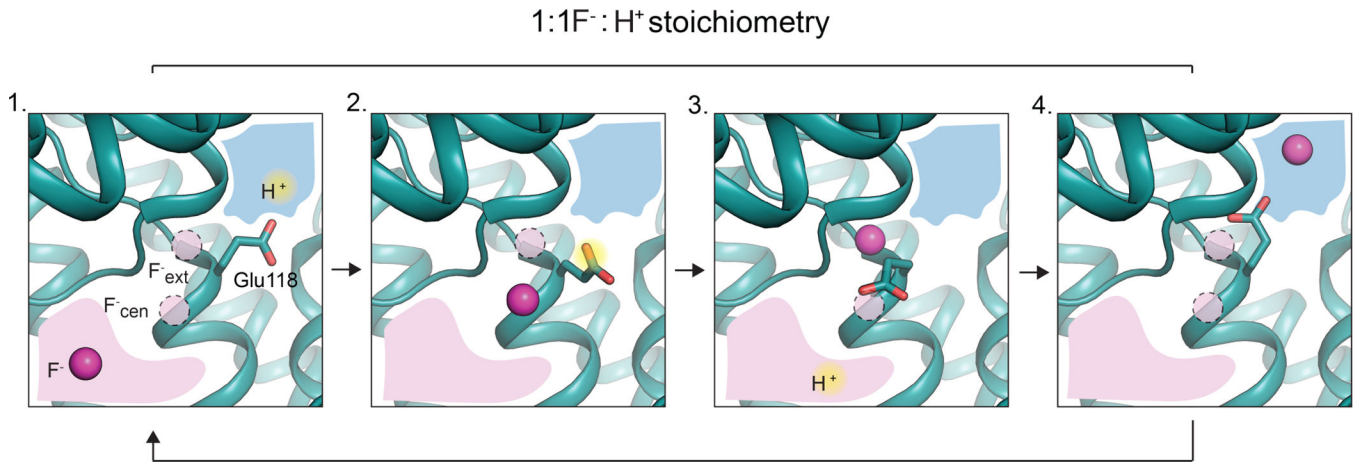

Figure 4. Proposed CLC^{F} transport mechanism.

The extracellular solution is shown in blue and the intracellular solution in pink. The gating glutamate E118 is shown in stick representation, and a yellow halo indicates protonation. The four steps of the fluoride/proton antiport cycle are described in the text. Fluoride ions are shown as pink spheres, and when unoccupied, fluoride binding sites are indicated with pink dashed circles.

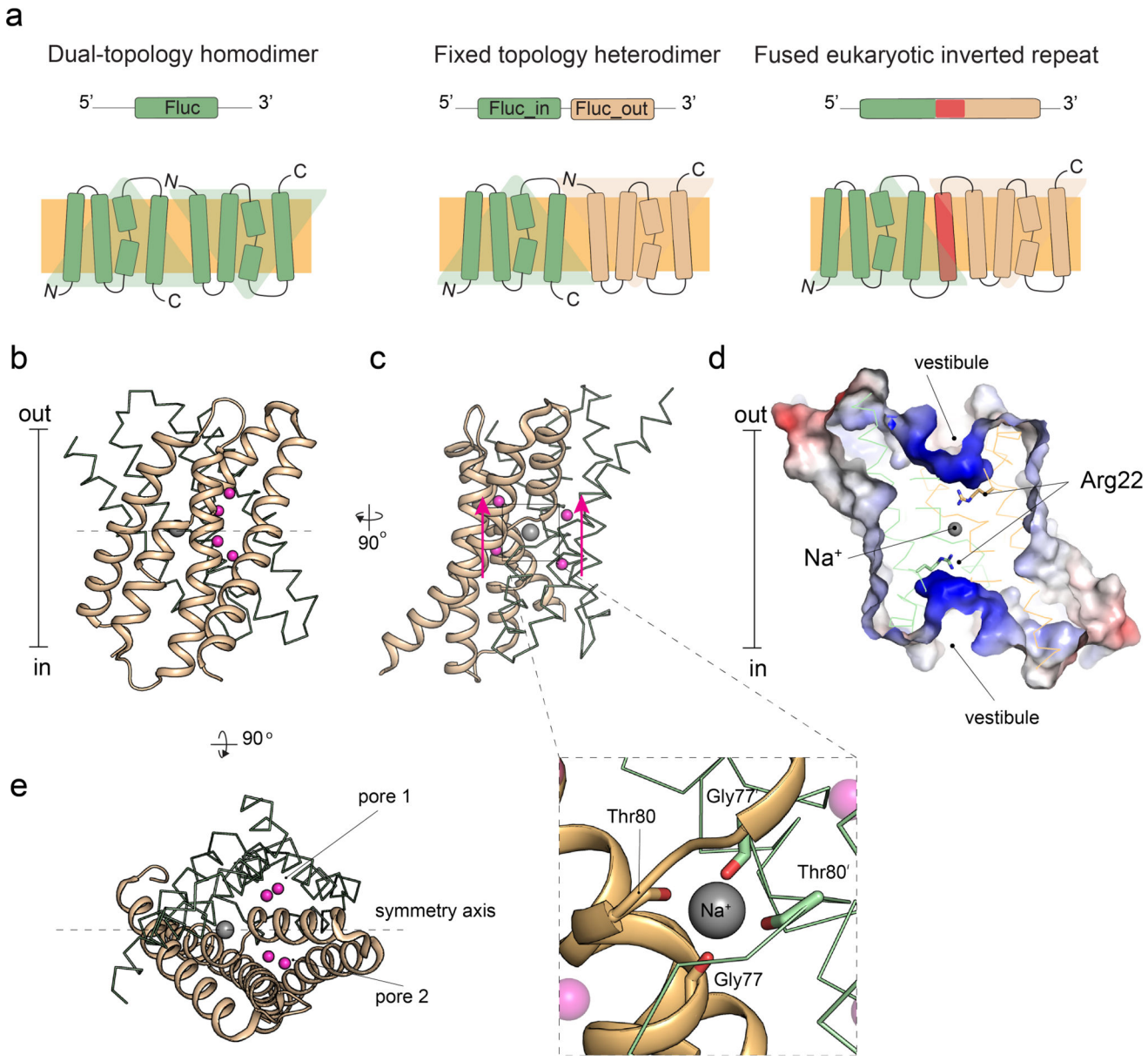

Figure 5. Fluoride channel architecture.

a. Fluoride channel topologies, including dual topology homodimers, antiparallel heterodimers, and inverted repeat monomers. Genetic architecture is shown at top, and resultant membrane topology is shown below. b. Structure of the Fluc-Bpe (PDB: 5NKQ). One monomer is rendered in cartoon format, and the other monomer rendered in ribbon format. Fluoride ions are shown as pink spheres. The two-fold symmetry axis is shown as a dashed line. c. View of Fluc dimer from (b) rotated 90° with the central Na^+ shown as a gray sphere. Arrows adjacent to the fluoride ions denote direction of fluoride movement along the two pores. Lower panel, zoomed-in view of the central Na^+ binding site, with the backbone atoms of coordinating residues shown as sticks. d. Fluc channel sliced at the midpoint along a plane perpendicular to the membrane with surface electrostatics shown. Electropositive

surfaces in blue. e. Top-down view of Fluc homodimer with two-fold symmetry axis shown as a dashed line.

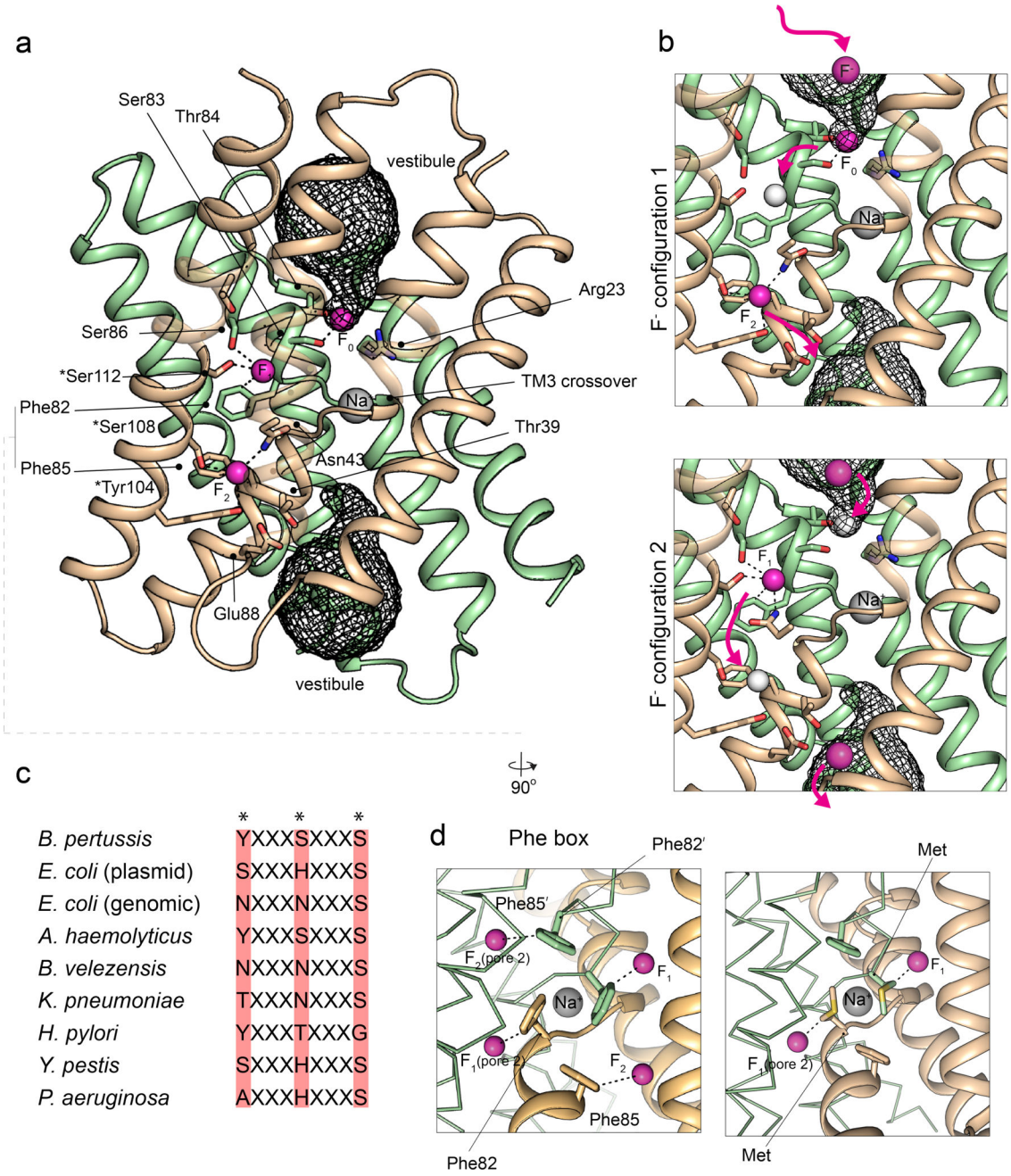

Figure 6. Proposed fluoride channel pore.

a. Compilation of structural data from Fluc-Bpe and Fluc-Ec2 showing fluoride binding sites F_0, F_1, and F_2 along the proposed fluoride permeation pathway. Numbering according to Fluc-Bpe, with mechanistically important sidechains shown as sticks and polar track residues indicated by asterisks. Subunits colored in tan and green with aqueous vestibules (determined by Caver (98)) shown as dark mesh. b. Proposed alternate occupancy of fluoride ions. The electrostatic repulsion that occurs between fluoride ions in adjacent sites contributes to rapid conduction. Zoomed-in views of fluoride binding configurations with occupied sites indicated in pink and unoccupied sites indicated in white. Fluoride ion

movement indicated with pink arrows. c. Sequence alignment of TM4 polar track from several microbial Fluc channels. d. Left, view of the phenylalanine box, with edge-on coordination of fluoride ions indicated with dashed lines. This view emphasizes the two-pore construction of the channel. Note that in panels (a) and (d), the ions in the F_1-pore 2 and F_2-pore 2 sites are omitted for clarity. Right, structure of Fluc-Ec2 mutant F82M (PDB: 6B2B), a fluoride-conducting phenylalanine box mutant.

Table 1.

Comparison of the physicochemical properties of fluoride and chloride.

	Radius (Å)(28)	**ΔG_{hyd} (kcal./mol)(29)**	**pK_a (conjugate acid)**	**Polarizability ($Å^3$)(30)**	**Preferred ligand number[1](31–34)**
F^-	1.31	−111.1	3.2	1.14	~4–7
Cl^-	1.88	−81.3	−7	3.25	~5–9

[1]Based on theoretical treatments of anion hydration and experimental observations from organic host-guest chemistry